

Vortex-lattice symmetry near T_c in $\text{YNi}_2\text{B}_2\text{C}$

C. D. Dewhurst,^{1,*} S. J. Levett,^{1,2,†} and D. McK. Paul²

¹*Institut Laue-Langevin, 6 rue Jules Horowitz, 38042 Grenoble, France*

²*Department of Physics, University of Warwick, Coventry CV4 7AL, United Kingdom*

(Received 31 March 2005; published 27 July 2005)

Detailed high-resolution small-angle neutron diffraction measurements have been used to determine the structural phase diagram of the vortex lattice (VL) in $\text{YNi}_2\text{B}_2\text{C}$ with $\mathbf{H}\parallel\mathbf{c}$. At low temperatures ($T\ll T_c$) the first-order 45° reorientation transition at a field $H_1(T)$ and second-order rhombic to square transition, $H_2(T)$ have previously been described by the effects of Fermi surface (FS) anisotropy and nonlocality. $H_1(T)$ decreases while $H_2(T)$ increases with increasing temperature. Measurements of the VL structure as close to the upper critical field $T_{c2}(H)$ as is currently experimentally feasible show no evidence of significant upward curvature or reentrance of H_2 that is expected when thermal fluctuations suppress nonlocality. For fields $H_1(T) < H < H_2(T)$ the VL remains rhombic and shows no sign of becoming hexagonal close to $T_{c2}(H)$. Our data suggest that an underlying electronic asymmetry, other than FS and nonlocal effects and likely due to an anisotropic superconducting gap, controls the VL structure close to $T_{c2}(H)$.

DOI: [10.1103/PhysRevB.72.014542](https://doi.org/10.1103/PhysRevB.72.014542)

PACS number(s): 74.25.Dw, 74.25.Ha, 74.70.Dd

The morphology of the vortex lattice (VL) in type-II superconductors continues to attract a great deal of interest due to the inherent correlation between the symmetry of the underlying electronic structure, details of the pairing mechanism, and the macroscopic physics of the VL.¹⁻⁹ Changes in symmetry and orientation of the VL can arise due to an underlying anisotropy of either the Fermi surface (FS) or superconducting energy gap. This comes about since the relation between the supercurrent and vector potential of the magnetic induction can be nonlocal, reflecting the finite spatial extent of the Cooper pair $\xi_0 = v_F / \pi \Delta_0$, where v_F is the Fermi velocity and Δ_0 is the superconducting gap at zero temperature. For “conventional” type-II superconductors ($\kappa > 1/\sqrt{2}$) with an isotropic gap such as Nb, PbTl, and V_3Si square or rhombic VL structures have been observed for magnetic fields applied along a fourfold symmetry axis.¹⁰⁻¹²

Kogan *et al.*^{5,6} have been able to describe the structure, orientation, and field dependence of the VL at low temperatures in cubic V_3Si (Ref. 12) and the tetragonal rare-earth borocarbides $\text{RNi}_2\text{B}_2\text{C}$ (Refs. 2 and 3) using nonlocal corrections to the London model and estimates for the relevant Fermi velocity averages. In borocarbide superconductors the (nearly) hexagonal VL undergoes a rhombic distortion with increasing field with the long diagonal along the $[110]$ direction. This means that the apex angle β is smaller than the usual 60° for a hexagonal VL [Fig. 1(a)]. At a field $H_1(T)$ the VL undergoes a first-order 45° reorientation and simultaneous jump in β to a value greater than 60° [Fig. 1(b)]. Increasing field distorts the VL further until a square lattice is formed above $H_2(T)$ via a continuous transition.¹⁻⁴ In Co-doped $\text{Lu}(\text{Ni}_{1-x}\text{Co}_x)_2\text{B}_2\text{C}$ increasing Co concentration decreases the mean free path l , reducing nonlocal effects, which in turn leads to a rise in $H_2(T)$.¹³ $H_2(T)$ also rises with increasing temperature, again roughly consistent with weakened nonlocality due to thermal fluctuations.³ DeWilde *et al.*¹ and Park and Huse⁷ have extended the Ginzburg-Landau (GL) description of the VL free energy by including fourfold symmetric terms which might arise due to either FS or gap

anisotropy. They suggest that $H_2(T)$ should rise with increasing temperature and make a finite intercept with the upper critical field $H_{c2}(T)$. By incorporating the effects of thermal fluctuations in the nonlocal London theory, Gurevich and Kogan⁸ find that, unlike the extended Ginzburg-Landau models,^{1,7} $H_2(T)$ and $H_{c2}(T)$ do not cross. Strong thermal fluctuations of vortices near $H_{c2}(T)$ are thought to suppress the anisotropy induced by the nonlocality resulting in a reentrance of the rhombic VL phase. This model was developed partly in response to the small-angle neutron diffraction data of Eskildsen *et al.*³ for $\text{LuNi}_2\text{B}_2\text{C}$ which appears to show significant upward curvature and even reentrance of $H_2(T)$.

If a superconductor exhibits nodes in the gap, as is thought to be the case for the cuprates ($\kappa \sim 50$), the effective coherence length $\xi_0 = v_f / \pi \Delta_0$ becomes angular dependent, diverging along the node directions. As pointed out by Franz *et al.*,¹⁶ this means that the condition $\kappa \gg 1/\sqrt{2}$ is no longer satisfied and superconductivity is effectively nonlocal along the nodal directions. Such corrections reflect the gap anisotropy and contribute to an anisotropic vortex-vortex interaction. Recent observation of a square VL in $\text{La}_{2-x}\text{Sr}_x\text{CuO}_{4+\delta}$,¹⁷ $\text{YBa}_2\text{Cu}_3\text{O}_{7-d}$,¹⁸ the electron-doped $\text{Nd}_{1.85}\text{Ce}_{0.15}\text{CuO}_4$,¹⁹ and heavy-fermion CeCoIn_5 (Ref. 20) have been presented as evidence for an anisotropic gap and d -wave pairing in these materials. There is now substantial evidence that the superconducting gap in $\text{YNi}_2\text{B}_2\text{C}$ is anisotropic, as demonstrated by specific heat,^{21,22} thermal conductivity,^{23,24} photoemission spectroscopy,²⁵ and point contact spectroscopy.^{26,27} Izawa *et al.*²⁴ used angular-resolved thermal conductivity measurements in a magnetic field to show that the superconducting gap in $\text{YNi}_2\text{B}_2\text{C}$ exhibits a fourfold symmetry and is significantly smaller in the $[100]$ direction than the $[110]$, consistent with point nodes along the directions of maximum v_F .²⁸ Also motivated by the apparently reentrant $H_2(T)$ in $\text{LuNi}_2\text{B}_2\text{C}$ Nakai *et al.*⁹ have investigated the case when both FS and gap anisotropies are present. They suggest that the competing anisotropies each promote the formation of a

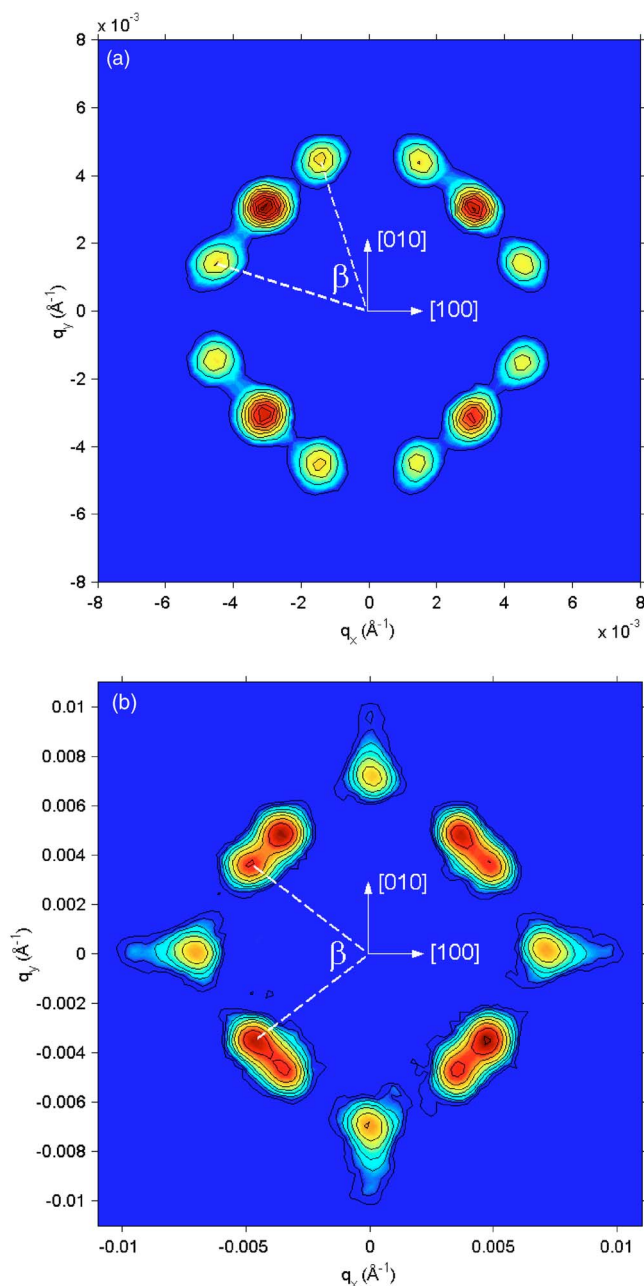


FIG. 1. (Color online) Small-angle diffraction from the VL in $\text{YNi}_2\text{B}_2\text{C}$ with $\mathbf{H}\parallel c$ at 4.5 K. (a) shows the low-field rhombic VL at 100 mT [$H(T) < H_1(T)$] while (b) shows the high-field rhombic VL at 170 mT [$H_1(T) < H < H_2(T)$]. The dashed lines indicate unit cell vectors of one VL domain in reciprocal space.

square VL, \square_v and \square_g , but mutually rotated by 45° . They also find that the boundary between \square_v and the hexagonal Δ_v phase [$H_2(T)$] may indeed exhibit upward curvature and reentrance, depending upon their choice of model parameters. In this paper we report small-angle neutron diffraction measurements of the VL in $\text{YNi}_2\text{B}_2\text{C}$ over a wide region of the magnetic field—temperature phase diagram and as close to $T_{c2}(H)$ as currently experimentally feasible in order to examine possible contributions to the VL structure from both FS and gap anisotropies.

Single crystals of $\text{YNi}_2^{11}\text{B}_2\text{C}$ [$T_c(0) \approx 15.8$ K] were

grown using a high-temperature flux method.²⁹ Small-angle neutron diffraction measurements were carried out using the D22 instrument at the Institut Laue-Langevin, Grenoble, France. Additional high-field data were collected using the SANS I instrument at the Paul Scherrer Institut, Villigen, Switzerland. The instruments were configured in a high-resolution mode with mean incident neutron wavelengths between 10 and 15 \AA and 10% wavelength spread with collimation defined by a variable diameter circular aperture and a 5 mm sample aperture separated by 18 m. The diffracted intensity was imaged using a 128×128 (7.5 mm^2) pixel area detector 18 m from the sample. The c axis of the crystal was aligned parallel to the magnetic field (to within 1°). The diffracted intensity from the VL is roughly proportional to $1/\lambda^4$, where λ is the London penetration depth, and hence decreases significantly at elevated temperatures. With the high incident flux available at D22 we were able to clearly detect scattering from the VL in the $\text{YNi}_2\text{B}_2\text{C}$ crystal (10 mg) up to $\approx 0.9T_c(H)$ with reasonable counting times. All measurements were made after field cooling (FC) followed by a small (10%) damped oscillation of the applied field to “post-anneal” the FC VL and better resolve the individual Bragg reflections.⁴

Typical small-angle neutron diffraction images from the VL in $\text{YNi}_2\text{B}_2\text{C}$ are shown in Fig. 1. Each image consists of the sum of counts obtained as the crystal and magnetic field are tilted horizontally and vertically to satisfy the Bragg condition for each of the first-order reflections. Two equivalent orientations of VL domains exist for this orientation of the applied field due to symmetry. Figure 1(a) shows the diffraction pattern at a low field ($H < H_1$) oriented with the diagonal of the rhombic VL unit cell along the crystal $[110]$ and with opening angle $\beta < 60^\circ$ ($\approx 54^\circ$). Figure 1(b) shows the diffraction pattern at higher fields $H_1 < H < H_2$, after the rhombic VL has reoriented by 45° and β has abruptly switched to a value greater than 60° . Unit cell diagonals are now along the $[100]$ and $[010]$ directions and $\beta \approx 82^\circ$. In Fig. 1(b) the first-order Bragg peaks are present in pairs, one from each of the orthogonal domains. The azimuthal splitting of these two first-order Bragg peaks is also visible in the higher-order (1,1) reflections which are consequently extended in the radial direction.

Data similar to that shown in Fig. 1 has been used to measure the VL orientation and distortion as a function of temperature and magnetic field. The apex angle β of each VL unit cell was determined by measuring the position of each reflection at its Bragg angle by multiple two-dimensional Gaussian fits to the multidetector data. Fitting a single function and monitoring the azimuthal width of the broadened first-order Bragg peaks is not an ideal test for small rhombic distortions since disordering due to pinning can also cause azimuthal broadening of the Bragg reflections. Monitoring the much weaker higher-order reflections, on the other hand, allows us to distinguish between broadening due to rhombic distortion and that due to disordering, since rhombic distortion alone should result in azimuthally broadened (1,0) reflections and radially broadened (1,1) reflections, as shown in Fig. 1(b).

Figure 2 shows β as a function of magnetic field for sev-

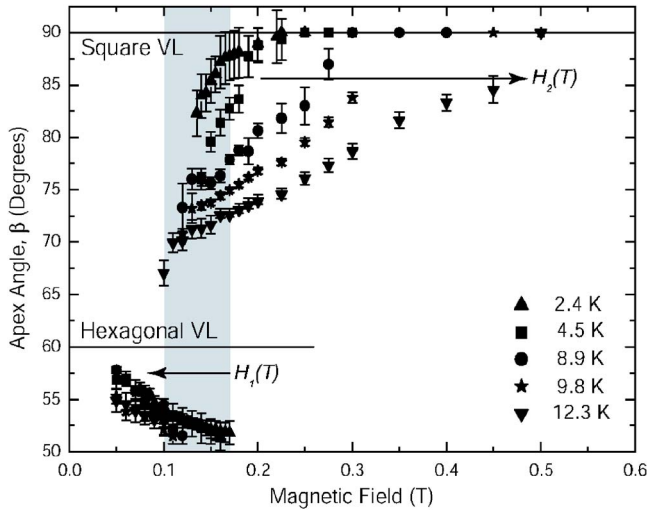


FIG. 2. (Color online) VL apex angle β vs magnetic field for temperatures between 2.4 and 12.3 K. $H_1(T)$ decreases while $H_2(T)$ increases with increasing temperature. The shaded area indicates the region of coexisting low- and high-field rhombic phases about the first order reorientation transition $H_1(T)$ (Ref. 4).

eral temperatures. The low-field rhombic phase corresponds to $\beta < 60^\circ$ while the high-field phase corresponds to $\beta > 60^\circ$. The general form of the data is remarkably similar to that calculated from the nonlocal London model by Kogan *et al.*⁶ whereby β initially decreases with increasing field before reorientation at $H_1(T)$. The shaded area close to H_1 indicates a region of coexisting low- and high-field phases, expected around a first-order transition in the presence of finite disorder (pinning).⁴ Above $H_1(T)$ the reoriented high-field rhombic structure distorts continuously from an angle greater than 60° toward 90° forming a square VL above the second-order $H_2(T)$. The phase diagram for $\text{YNi}_2\text{B}_2\text{C}$ as determined from our small-angle diffraction data is shown in Fig. 3. The upper critical field $H_{c2}(T)$ was determined by *dc* magnetization measurements on the same single crystal. The square symbols \square_v indicate where we have identified a square VL close to, but just above $H_2(T)$ at high temperatures and in fields of up to 3.75 T at 1.8 K. Also shown schematically in Fig. 3 are contours of constant β estimated from our diffraction data measured at discrete field and temperature points. Figures 2 and 3 show that $H_1(T)$ gradually decreases while the transition to a square VL at $H_2(T)$ increases with increasing temperature. This means that the region of the magnetic phase diagram over which the high-field rhombic VL phase occurs “expands” at higher temperatures. In other words, larger distortions of the high-field rhombus are supported rather than the square or low-field rhombic phase as $H_{c2}(T)$ is approached.

Accurate determination of $H_2(T)$ and $H_1(T)$ becomes increasingly difficult at higher temperatures due to the weak diffracted intensity from the VL and at low fields due to disordering effects (pinning).^{30,31} The temperature dependence of $H_2(T)$ presented in Fig. 3 shows no indication of significant upward curvature or reentrance as far as we are able to measure close to $T_{c2}(H)$. It is reasonable to expect that both the Y and Lu borocarbides are almost identical

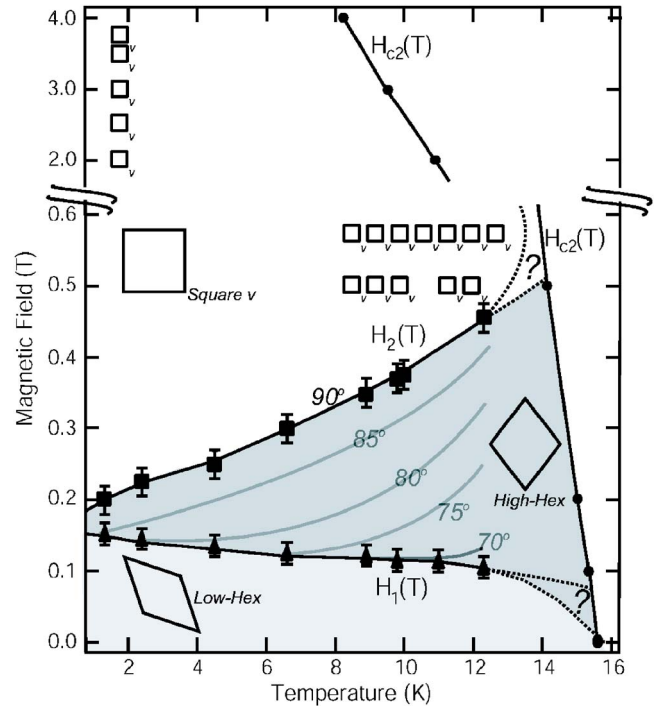


FIG. 3. (Color online) Phase diagram for $\text{YNi}_2\text{B}_2\text{C}$ for $\mathbf{H} \parallel \mathbf{c}$ as derived from our neutron diffraction and *dc* magnetization measurements. Schematic contours of constant VL angle β estimated from our data are also shown. The symbols \square_v indicate observations of a square VL.

superconductors and should have rather similar superconducting parameters and phase diagrams. It is surprising, therefore, that our data for $\text{YNi}_2\text{B}_2\text{C}$ ($T_c \approx 15.8$ K) and the $\text{LuNi}_2\text{B}_2\text{C}$ ($T_c \approx 16.6$ K) data³ should apparently be so different. By monitoring the width of the broadened first order Bragg peaks Eskildsen *et al.*³ determined $H_2(T)$ and contours corresponding to a splitting angle away from a square VL. They chose to identify $H_2(T)$ by defining a Bragg peak splitting criterion of 3° . $H_2(T)$ determined in this way exhibits strong upward curvature and even reentrance, well below T_c , above ≈ 10 K ($\approx 0.60T_c$). Contours corresponding to larger Bragg peak splitting, on the other hand, exhibit a much weaker upward curvature and do not show signs of reentrance. It is useful to note that the high flux and resolution of the D22 instrument used for our measurements has allowed us to work with a much smaller, more perfect single crystal of $\text{YNi}_2\text{B}_2\text{C}$, rather than the larger ($\times 100$) mosaic of naturally-aligned $\text{LuNi}_2\text{B}_2\text{C}$ crystallites used in Ref. 3. We have also made some small-angle neutron scattering (SANS) measurements of the VL on the same $\text{LuNi}_2\text{B}_2\text{C}$ crystal used by Eskildsen *et al.* These data clearly show a significant disordering of the VL at low fields,³⁰ much more so than our equivalent measurements of $\text{YNi}_2\text{B}_2\text{C}$ presented here and in Ref. 4. We believe therefore that our crystal exhibits much weaker disordering effects due to pinning or surface effects³¹ and smaller crystals allow us to use our VL postannealing technique requiring only relatively small *ac* field oscillations.⁴ It is possible that their apparent reentrance of $H_2(T)$ may be convoluted with disordering such as due to the

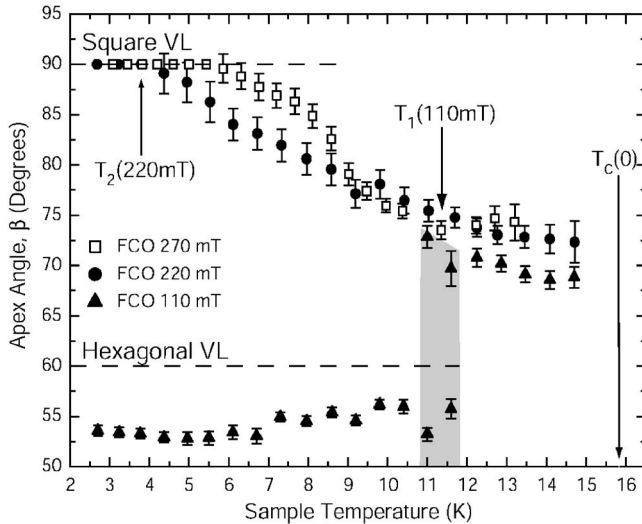


FIG. 4. VL apex angle β vs temperature for magnetic fields of 110, 220, and 270 mT. The shaded area represents the region of coexistence of the high- and low-field phases though the $H_1(T)$ transition at ≈ 11.5 K, 110 mT.

peak effect,^{32,33} and instrument resolution limitations.

The form of our $H_2(T)$ data makes it tempting to extrapolate $H_2(T)$ to form a finite intercept with $H_{c2}(T)$, in a manner similar to that suggested by the GL approach incorporating higher-order terms of either FS or gap anisotropy origin.^{1,7} While we do not have experimental data for $H_2(T)$ for temperatures greater than 12.3 K [$0.8T_{c2}(0.5T)$], Fig. 3 shows \square_v points where we have positively identified a square VL close to but just above $H_2(T)$. This sets much tighter limits as to where, if at all, $H_2(T)$ may upturn or be reentrant. On the other hand since it is widely accepted that the low-temperature behavior can be described by the nonlocal London model,⁶ it seems reasonable to incorporate thermal fluctuations.⁸ The model parameters required to locate $H_2(T)$ to coincide with experimental data for $\text{LuNi}_2\text{B}_2\text{C}$ are rather unphysical¹⁴ but the fit yields more reasonable parameters when compared to the recent experimental data for V_3Si .¹⁵ The VL phase diagram for V_3Si rather convincingly demonstrates a reentrant rhombic-square boundary, turning upward sharply above ≈ 10 K ($\approx 0.61T_c$).¹⁵ Interestingly the V_3Si data exhibits a phase diagram where the low-field rhombic phase transforms *directly* into the square phase via a first order transition. Thus, V_3Si does not exhibit the high-field rhombic phase at all demonstrating at least one distinctive difference in vortex behavior and underlying superconducting properties between V_3Si and the borocarbides. A similar absence of the high-field rhombic phase has also been noted in studies of $\text{Ca}_3\text{Rh}_4\text{Sn}_{13}$.³⁴

Finally, in Fig. 4, we show β determined from data measured as the FC VL is warmed from low to high temperatures. For 110 mT and low temperatures the VL is in the low-field rhombic phase. As $H_1(T)$ is crossed with increasing temperature at ≈ 11.5 K the VL reorients to the high-field rhombus with $\beta \approx 70^\circ$. At 210 and 270 mT the VL begins

square and crosses $H_2(T)$ into the high-field rhombus with β decreasing continuously with increasing temperature. Closer inspection of Fig. 4 reveals that β appears to saturate at the highest temperatures to a value close to 70° and does not tend toward 60° and a hexagonal VL, at least to within 1 K of $T_c(H)$. If nonlocality alone were responsible for the observed VL structure then as thermal fluctuations suppress these effects a hexagonal VL oriented with nearest neighbors along the crystal $[100]$ direction should be formed. At the same time it is assumed that nonlocal effects also become unimportant for large intervortex spacings ($> \lambda$) at low fields where we clearly observe the low-field rhombic phase tending toward hexagonal but oriented differently with nearest neighbors along the crystal $[110]$ direction. These two scenarios appear to be inconsistent if the weakened nonlocality leads to different orientations of the VL at high temperatures or low fields. It is therefore difficult to speculate as to the locus of $H_1(T)$ for temperatures approaching T_c as to whether it should intercept $H_{c2}(T)$ at finite or zero field. It is useful to contrast once more with the data for V_3Si where the high-field rhombic phase does not exist and instead the square lattice always reverts back to the low-field rhombus (first order) as $T_c(H)$ is approached.¹⁵

A key question therefore is why does $H_2(T)$ show no sign of significant upward curvature or reentrance as $T_{c2}(H)$ is approached? Our data for $\text{YNi}_2\text{B}_2\text{C}$ show that the high-field rhombic VL appears to saturate with β close to $\approx 70^\circ$ for temperatures approaching $T_{c2}(H)$. The VL does not tend toward hexagonal with either the low- or high-field orientations. Another fundamental question is why the high-field rhombic VL phase is present in the borocarbides and CeCoIn_5 (Ref. 35) but is apparently absent in the conventional (but nonlocal) superconductors V_3Si and $\text{Ca}_3\text{Rh}_4\text{Sn}_{13}$. We believe that the key difference between these systems is that the borocarbides and CeCoIn_5 are materials where the order parameter is thought to be highly anisotropic.

Nakai *et al.*⁹ have used the Eilenberger theory in an attempt to describe the competition between superconducting gap and FS anisotropies for superconductors with fourfold symmetry. Here the sense of the two anisotropies are such that square VL associated with FS or gap anisotropy are mutually oriented by 45° , as is the case for borocarbide superconductors. As nonlocality weakens at higher temperatures and core interactions dominate at high fields they propose that it is the gap asymmetry that becomes dominant promoting a square \square_g VL oriented at 45° to the \square_v we observed up to 3.75 T [$\approx 0.4B_{c2}(0)$] (Fig. 3). They also find that the boundary from rhombic to square ($H_2(T)$) should exhibit upward curvature and a complete reentrance due to the competition between gap and FS anisotropies as well as thermal fluctuations. At high temperatures and low fields they find that a hexagonal VL should be present but cannot determine its orientation or take account of rhombic distortions. They do not produce or discuss the low-field rhombic state [$< H_1(T)$] or its orientation. While our data for $\text{YNi}_2\text{B}_2\text{C}$ are not described well by this model we suggest that there is a lasting underlying fourfold anisotropy, different to and combined with the anisotropic FS and nonlocality in the borocarbide superconductors that is robust up to $T_c(H)$ and domi-

nates the high-temperature region of the magnetic phase diagram. Further theoretical consideration needs to be given to anisotropies from FS and gap symmetry and the effects of thermal fluctuations if the phase diagram is to be successfully described.

In summary, we have made detailed small-angle neutron diffraction measurements of the VL structure and orientation in $\text{YNi}_2\text{B}_2\text{C}$ as a function of temperature and magnetic field. The first-order reorientation transition of the rhombic VL, $H_1(T)$, *decreases* while the second-order transition to a square VL, $H_2(T)$, *increases* with increasing temperature. We find no substantive evidence to show that $H_2(T)$ curves upward or becomes reentrant for temperatures approaching $T_{c2}(H)$ which might be expected when thermal fluctuations

suppress nonlocal effects at high temperatures. We argue that the expanding high-field rhombic region of the magnetic phase diagram at high temperatures is inconsistent with the VL structure and orientation being determined by Fermi surface anisotropy and nonlocality alone. It seems likely that the anisotropic superconducting gap in the borocarbides plays an additional important role in determination of the VL morphology.

We would like to thank Morten Eskildsen, Mohana Yethiraj, Vladimir Kogan, and Alex Gurevich for valuable discussions. Thanks also to Joachim Kohlbrecher and staff at PSI Switzerland who assisted with the high-field SANS measurements.

*Electronic address: dewhurst@ill.fr

[†]Present address: ISIS Facility, Rutherford Appleton Laboratory, Chilton, Didcot, OX11 0QX, U.K.

¹Y. DeWilde, M. Iavarone, U. Welp, V. Metlushko, A. E. Koshelev, I. Aranson, G. W. Crabtree, and P. C. Canfield, *Phys. Rev. Lett.* **78**, 4273 (1997).

²D. McK. Paul, C. V. Tomy, C. M. Aegerter, R. Cubitt, S. H. Lloyd, E. M. Forgan, S. L. Lee, and M. Yethiraj, *Phys. Rev. Lett.* **80**, 1517 (1998).

³M. R. Eskildsen, A. B. Abrahamsen, V. G. Kogan, P. L. Gammel, K. Mortensen, N. H. Andersen, and P. C. Canfield, *Phys. Rev. Lett.* **86**, 5148 (2001).

⁴S. J. Levet, C. D. Dewhurst, and D. McK. Paul, *Phys. Rev. B* **66**, 014515 (2002).

⁵V. G. Kogan, P. Miranović, L. Dobrosavljević-Grujić, W. E. Pickett, and D. K. Christen, *Phys. Rev. Lett.* **79**, 741 (1997).

⁶V. G. Kogan, M. Bullock, B. Harmon, P. Miranović, L. Dobrosavljević-Grujić, P. L. Gammel, and D. J. Bishop, *Phys. Rev. B* **55**, R8693 (1997).

⁷K. Park and D. A. Huse, *Phys. Rev. B* **58**, 9427 (1998).

⁸A. Gurevich and V. G. Kogan, *Phys. Rev. Lett.* **87**, 177009 (2001).

⁹N. Nakai, P. Miranović, M. Ichioka, and K. Machida, *Phys. Rev. Lett.* **89**, 237004 (2002).

¹⁰D. K. Christen, H. R. Kerchner, S. T. Sekula, and P. Thorel, *Phys. Rev. B* **21**, 102 (1980).

¹¹B. Obst, *Phys. Lett.* **28A**, 662 (1969).

¹²M. Yethiraj, D. K. Christen, D. McK. Paul, P. Miranović, and J. R. Thompson, *Phys. Rev. Lett.* **82**, 5112 (1999).

¹³P. L. Gammel, D. J. Bishop, M. R. Eskildsen, K. Mortensen, N. H. Andersen, I. R. Fisher, K. O. Cheon, P. C. Canfield, and V. G. Kogan, *Phys. Rev. Lett.* **82**, 4082 (1999).

¹⁴A. Gurevich (private communication).

¹⁵M. Yethiraj, D. K. Christen, A. A. Gapud, D. McK. Paul, S. Crowe, C. D. Dewhurst, R. Cubitt, L. Porcar, and A. Gurevich (unpublished).

¹⁶M. Franz, I. Affleck, and M. H. S. Amin, *Phys. Rev. Lett.* **79**, 1555 (1997).

¹⁷R. Gilardi, J. Mesot, A. Drew, U. Divakar, S. L. Lee, E. M. Forgan, O. Zaharko, K. Conder, V. K. Aswal, C. D. Dewhurst, R. Cubitt, N. Momono, and M. Oda, *Phys. Rev. Lett.* **88**,

217003 (2002).

¹⁸S. P. Brown, D. Charalambous, E. C. Jones, E. M. Forgan, P. G. Kealey, A. Erb, and J. Kohlbrecher, *Phys. Rev. Lett.* **92**, 067004 (2004).

¹⁹R. Gilardi, J. Mesot, S. P. Brown, E. M. Forgan, A. Drew, S. L. Lee, R. Cubitt, C. D. Dewhurst, T. Uefuji, and K. Yamada, *Phys. Rev. Lett.* **93**, 217001 (2004).

²⁰M. R. Eskildsen, C. D. Dewhurst, B. W. Hoogenboom, C. Petrovic, and P. C. Canfield, *Phys. Rev. Lett.* **90**, 187001 (2003).

²¹K. Izawa, A. Shibata, Y. Matsuda, Y. Kato, H. Takeya, K. Hirata, C. J. van der Beek, and M. Konczykowski, *Phys. Rev. Lett.* **86**, 1327 (2001).

²²T. Park, M. B. Salamon, E. M. Choi, H. J. Kim, and S. I. Lee, *Phys. Rev. Lett.* **90**, 177001 (2003).

²³E. Boaknin, R. W. Hill, C. Proust, C. Lupien, L. Taillefer, and P. C. Canfield, *Phys. Rev. Lett.* **87**, 237001 (2001).

²⁴K. Izawa, K. Kamata, Y. Nakajima, Y. Matsuda, T. Watanabe, M. Nohara, H. Takagi, P. Thalmeier, and K. Maki, *Phys. Rev. Lett.* **89**, 137006 (2002).

²⁵T. Yokoya, T. Kiss, T. Watanabe, S. Shin, M. Nohara, H. Takagi, and T. Oguchi, *Phys. Rev. Lett.* **85**, 4952 (2000).

²⁶P. Raychaudhuri, D. Jaiswal-Nagar, G. Sheet, S. Ramakrishnan, and H. Takeya, *Phys. Rev. Lett.* **93**, 156802 (2004).

²⁷H. Nishimori, K. Uchiyama, S. Kaneko, A. Tokura, H. Takeya, K. Hirata, and N. Nishida, *J. Phys. Soc. Jpn.* **73**, 3247 (2004).

²⁸S. B. Dugdale, M. A. Alam, I. Wilkinson, R. J. Hughes, I. R. Fisher, P. C. Canfield, T. Jarlborg, and G. Santi, *Phys. Rev. Lett.* **83**, 4824 (1999).

²⁹B. K. Cho, P. C. Canfield, L. L. Miller, D. C. Johnston, W. P. Beyermann, and A. Yatskar, *Phys. Rev. B* **52**, 3684 (1995).

³⁰C. D. Dewhurst (unpublished).

³¹S. S. James, C. D. Dewhurst, R. A. Doyle, D. McK. Paul, Y. Paltiel, E. Zeldov, and A. M. Campbell, *Physica C* **332**, 173 (2000).

³²M. R. Eskildsen, P. L. Gammel, B. P. Barber, A. P. Ramirez, D. J. Bishop, N. H. Andersen, K. Mortensen, C. A. Bolle, C. M. Lieber, and P. C. Canfield, *Phys. Rev. Lett.* **79**, 487 (1997).

³³V. N. Narozhnyi, G. Fuchs, K. Nenkov, D. Eckert, A. Teresiak, K.-H. Müller, and P. C. Canfield, *Physica C* **341**, 1141 (2000).

³⁴S. J. Levet, Ph.D. thesis, University of Warwick, 2002.

³⁵M. R. Eskildsen (private communications).